7,12-Dimethylbenz(*a*)Anthracene Treatment of a *c-rel* Mouse Mammary Tumor Cell Line Induces Epithelial to Mesenchymal Transition via Activation of Nuclear Factor-κB

Sangmin Ryan Shin,[1,3] Nuria Sánchez-Velar,[1,3] David H. Sherr,[2,3] and Gail E. Sonenshein[1,3]

Departments of [1]Biochemistry and [2]Environmental Health, Boston University Medical Campus and [3]Women's Health Interdisciplinary Research Center, Boston, Massachusetts

Abstract

The aberrant expression of the nuclear factor-κB (NF-κB) c-Rel subunit that occurs in many human breast cancers can play a causal role in tumorigenesis as judged by findings with a mouse mammary tumor virus (MMTV)-c-*rel* transgenic mouse model, in which 31.6% of mice developed one or more mammary tumors after a long latency. Interestingly, none of the cell lines established from the mammary tumors grew in soft agar. To begin to test the hypothesis that a prototypic carcinogen insult can promote a more invasive, mesenchymal phenotype, a cell line established from a MMTV-c-*rel* mammary tumor rel-3983 was treated in culture with the polycyclic aromatic hydrocarbon 7,12-dimethylbenz(a)anthracene (DMBA; rel-3983D cells) or DMSO vehicle (rel-3983V cells). Rel-3983D cells displayed an increased rate of proliferation, displayed growth to a higher cell density, and acquired the ability to grow in soft agar and in Matrigel compared with the parental rel-3983 or vehicle-treated rel-3983V cells. Consistent with a more mesenchymal phenotype, rel-3983D cells showed loss of E-cadherin expression as judged by immunofluorescence microscopy. Compared with control cells, rel-3983D displayed increased NF-κB binding and higher levels of the NF-κB transactivating subunits c-Rel, RelA, and RelB, which seemed functional as judged by induction of c-Myc and vimentin, products of two NF-κB target genes. Ectopic expression of a super repressor mutant of IκB-α reduced rel-3983D cell growth and invasive morphology in Matrigel, confirming the role of NF-κB in epithelial to mesenchymal transition (EMT). Thus, DMBA treatment of c-Rel–transformed mammary tumor cells in culture is shown here for the first time to result in EMT via activation of NF-κB. The aberrant c-Rel expression present in most human breast cancers suggests that this mechanism may play an important role in carcinogenesis. (Cancer Res 2006; 66(5): 2570-5)

Introduction

Breast cancer is the second leading cancer-related cause of death of women in the United States, where the incidence of late-onset breast cancer has been increasing since the 1980s. It has been estimated that known genetic risk factors, such as germ line mutation of identified breast cancer predisposition genes [e.g., *BRCA-1* (chromosome 17q21) and *BRCA-2* (chromosome 13q12-13)], account for only ~5% to 10% of breast cancer cases, which tend to be early onset. The remaining ~90% of breast cancers are late onset and arise from somatic genetic abnormalities (e.g., loss of tumor suppressor function or mutations in oncogenes). The recent increase in breast cancer incidence has led to the hypothesis that it results, in part, from increased exposure to and bioaccumulation of lipophilic environmental pollutants, such as polycyclic aromatic hydrocarbons (PAH; ref. 1). This hypothesis is based on epidemiologic studies relating increased breast cancer to carcinogen exposure (2, 3) and from studies showing increased levels of aromatic hydrocarbons and their receptors in breast carcinomas (4, 5) and in sera from breast cancer patients (3). In addition, PAH induce mammary tumorigenesis in rodent models (6) and transform mammary epithelial cells in culture (e.g., MCF-10F) yielding malignant cell lines (e.g., D3-1; ref. 7).

Interestingly, we have shown that nuclear factor-κB (NF-κB) is constitutively activated in breast cancer cells (8–10). NF-κB is a structurally and evolutionary conserved family of transcription factors distinguished by the presence of a 300-amino-acid region, termed the Rel homology domain (RHD), based on its homology with v-Rel, the transforming protein encoded by the RevT avian retrovirus. The RHD is responsible for DNA binding, dimerization, nuclear translocation, and interaction with the IκB inhibitory proteins (11). Mammals express five NF-κB members RelA (p65), RelB, c-Rel, NF-κB_1 (p50/p105), and NF-κB_2 (p52/p100). In most untransformed cells, other than B lymphocytes, NF-κB complexes are sequestered in the cytoplasm bound to specific inhibitory proteins, of which IκB-α is the paradigm. Activation of NF-κB involves phosphorylation and rapid degradation of IκB, allowing for translocation of free NF-κB to the nucleus, where it controls genes involved in cell growth, survival, adhesion, and immune and inflammatory responses, including *cyclin D1, c-myc, bcl-xl*, and *vimentin* (12, 13). Evidence from several laboratories has suggested that NF-κB is critically involved in the regulation of mammary tumorigenesis. For example, we have shown aberrant constitutive activation of NF-κB factors in the majority of primary human breast cancer specimens (e.g., 20 of 23 samples displayed nuclear c-Rel; ref. 8). High levels of nuclear NF-κB were similarly found in human and rodent breast cancer cell lines, including 7,12-dimethylbenz(*a*)anthracene (DMBA)–induced D3-1 cells (8, 9). Moreover, mammary tumors that developed in Sprague-Dawley female rats treated with a single dose of DMBA displayed induction of NF-κB binding (8). Accelerated degradation of the IκB-α inhibitory protein was observed in mammary epithelial cell lines transformed *in vitro* with DMBA (10). Importantly, inhibition of the constitutive NF-κB activity in human breast cancer cell lines induced apoptosis (8) or led to reduced tumorigenicity (14), suggesting a functional role of NF-κB in breast cancer. Because a large number of primary human breast cancer tissues examined

Requests for reprints: Gail E. Sonenshein, Department of Biochemistry, Boston University School of Medicine, 715 Albany Street, Boston, MA 02118. Phone: 617-638-4120; Fax: 617-638-4252; E-mail: gsonensh@bu.edu.

doi:10.1158/0008-5472.CAN-05-3056

expressed high levels of nuclear c-Rel (8, 15), we made a mouse mammary tumor virus (MMTV)-c-*rel* transgenic mouse model to test directly its role in breast cancer. Our studies showed a causal role for c-Rel: 31.6% of mice developed one or more mammary tumors, of diverse histology, at an average age of 19.9 months (16).

Carcinomas *in situ* progress to a more malignant phenotype via a process termed epithelial to mesenchymal transition (EMT), in which cells with an epithelial phenotype become more malignant or invasive taking on features of mesenchymal cells (17). During EMT, cancer cells lose expression of proteins that promote cell-cell contact, such as E-cadherin and β-catenin. The loss of E-cadherin is a hallmark of EMT and indicates progression to an invasive carcinoma (18). To test the hypothesis that PAH carcinogenesis can promote transition of a c-Rel overexpressing cell from an epithelial to mesenchymal phenotype, we treated a cell line derived from a mammary adenosquamous carcinoma in a MMTV-c-*rel* mouse in culture with 10^{-6} mol/L DMBA for 2 weeks. Cells were isolated with a highly invasive phenotype, displaying decreased E-cadherin expression, increased ability to grow in soft agar and Matrigel, and elevated levels of NF-κB. Importantly, the inhibition of NF-κB reduced invasive properties, indicating a critical role of NF-κB in carcinogen-induced EMT.

Materials and Methods

Transgenic mouse cell lines. Mammary tumor 3983 (adenosquamous cell carcinoma) from the MMTV-c-*rel* mouse line 14 was derived by explant. Briefly, tumor tissue was washed with sterile PBS and transferred to a P100 plate containing 10 mL fresh media: DMEM, containing 4.5 g/L D-glucose, 2.88 g/L $NaHCO_3$, supplemented with 3.25 mL/L of 200 mmol/L glutamine, 10% heat-inactivated fetal bovine serum, 100 μg/mL streptomycin, and 100 units/mL penicillin (all from Life Technologies/Invitrogen, Carlsbad, CA). The tumor tissue was minced into small pieces using two sterile pipette tips and incubated at 37°C, and the attachment of the cells was monitored. When most cells were attached and growing, the cells were washed with PBS and refed. Following passage, stock cultures were frozen.

The cell line derived from MMTV-c-*rel* line 14 #3983 tumor (rel-3983) was subjected to treatment with 10^{-6} mol/L DMBA dissolved in DMSO (rel-3983D) or DMSO vehicle (rel-3983V) for 2 weeks. Following treatment, cells were cultured and tested periodically for ability to grow in soft agar. After 60 passages, rel-3983D cells acquired the ability to grow in soft agar, whereas the parental (rel-3983) or vehicle-treated (rel-3983V) cells did not.

For growth curve analysis, cells were plated at 3,000/mL in six-well flat-bottomed plates in triplicate, incubated for the indicated number of days, trypsinized, and counted. NMuMG is an untransformed, immortalized mouse mammary epithelial cell line and was cultured as described previously (19).

Electrophoretic mobility shift analysis. Nuclear extracts were prepared, as we have described previously (16). Protein concentration was determined using the Bio-Rad protein assay, following the manufacturer's directions (Bio-Rad Laboratories, Richmond, CA). The sequence of the URE NF-κB–containing oligonucleotide from the *c-myc* gene (20) is as follows: 5′-GATCCAAGTCCGGGTTTTCCCCAACC-3′, where the underlined region indicates the core-binding element. The octomer-1 oligonucleotide has the following sequence: 5′-TGTCGAATGCAAATCACTAGAA-3′. Oligonucleotides were end labeled with large Klenow fragment of DNA polymerase and [^{32}P]deoxynucleotide triphosphates. The electrophoretic mobility shift assay (EMSA) was done as we have described previously (16).

Growth in soft agar. Sea plaque agarose (FMC Bioproducts, Rockland, ME), 1.6% by weight, was melted in double-distilled water by autoclaving for 30 minutes. Base agar was made by adding an equal volume of agarose solution and 2× DMEM with 20% heat-inactivated fetal bovine serum, 100 μg/mL streptomycin, 100 units/mL penicillin, and 1.5 mL of base agar was added to P35 Petri dishes. The top agar was prepared as above, except for addition of 5,000 cells per dish. Plates, prepared in triplicate, were incubated at 37°C for 14 days and photographed, as described previously (21).

Immunofluorescence analysis. Cells were grown on glass coverslips, fixed by incubation at room temperature in 2% electron microscopy-grade paraformaldehyde (EMS, Fort Washington, PA), 1× PBS, 5 mmol/L $MgCl_2$ (15 minutes), and permeabilized with 0.5% Triton X-100 in PBS. Cells were blocked by incubation in 2% (w/v) bovine serum albumin (Sigma, St. Louis, MO) in PBS (Buffer A) and incubated for 1 hour in primary antibody (mouse anti-E-cadherin; BD Biosciences, San Jose, CA) diluted in Buffer A. Following washing, the coverslips were incubated for 1 hour in anti-mouse Alexa 594 secondary antibodies (Life Technologies/Invitrogen) diluted in Buffer A. Following washing, the coverslips were mounted in Vectashield with 4′,6-diamidino-2-phenylindole (DAPI; H-1200, Vector Laboratories, Inc., Burlingame, CA). Fluorescence microscopy was done using a Zeiss Axiovert 200 M microscope. The images are representative of two independent experiments done in duplicate.

Preparation of nuclear and cytoplasmic extracts for immunoblot analysis. Washed cells were lysed by suspension for 15 minutes in ice-cold lysis buffer [10 mmol/L Tris (pH 7.6), 10 mmol/L KCl, 5 mmol/L $MgCl_2$] plus DTT, phenylmethlsulfonylfluoride, leupeptin, and 1% NP40. Lysis was assessed by crystal violet staining. The nuclei were pelleted by centrifugation for 4 minutes at 2,500 rpm at 4°C, and the supernatant containing cytoplasmic proteins was isolated. The nuclear pellets were washed once in lysis buffer without detergent and centrifuged, and proteins were extracted in 50 mmol/L Tris-HCl (pH 7.5), 150 mmol/L NaCl, 1% sodium lauryl sarcosine, 1% NP40, 0.1% SDS, 1 mmol/L EDTA plus DTT, phenylmethlsulfonylfluoride, and leupeptin as above. The DNA was sheared by passing the suspension first through a 23G and then a 25G7/8 needle. Following centrifugation for 30 minutes at 14,000 × *g* at 4°C, the supernatant containing the nuclear proteins was removed. Protein concentrations were determined using the Bio-Rad detergent-compatible protein assay, as described above.

Immunoblot analysis. Samples (40 μg) were separated by electrophoresis in 10% polyacrylamide-SDS gels, transferred to a 0.45-μm-pore polyvinylidene difluoride membrane (Millipore, Bedford, MA) and subjected to immunoblotting, as described (8). NF-κB antibodies included RelA (SC372), c-Rel (SC071), and RelB (SC226; all from Santa Cruz Biotechnology, Santa Cruz, CA); c-Myc antibody (786-5) was kindly provided by S. Hann (Vanderbilt University, Nashville TN); vimentin (MS-129-Pl) and β-actin (A-5441) antibody were purchased from Neomakers (Fremont, CA) and Sigma, respectively.

Matrigel assay. Matrigel was diluted to a concentration of 6.3 mg/mL with serum-free medium (DMEM) and stored at −80°C. Before use, samples were thawed on ice overnight. For the bottom layer, 200 μL of Matrigel solution was added into a 24-well tissue culture plate and incubated at 37°C for 30 minutes to allow the Matrigel to solidify. A single-cell suspension (5×10^5 cells/mL) in serum-free medium (DMEM) was made by passing the cell suspension through a 21(1/2) gauge needle five times. Ten microliters (5,000 cells) were mixed with 190 μL of Matrigel and plated, in duplicate, onto the solidified bottom layer. The plates were incubated at 37°C for 30 minutes to allow the Matrigel to solidify, and complete medium was then added. Following incubation at 37°C for 5 to 7 days, the cell growth was analyzed using a Zeiss Axiovert 200 M microscope.

Retroviral gene delivery. The pBABE-puro-Super Repressor (SR)-IκB-α construct, which expresses an IκB-α Ser32/36A mutant protein, was kindly provided by R. Romieu-Mourez (Boston University School of Medicine, Boston MA). The control pBABE-puro, which expresses green fluorescent protein (GFP), was described previously (22). Phoenix packaging cells were used for generation of retrovirus, using 500 μg/mL hygromycin selection to increase Gag and Pol viral protein expression. Briefly, P100 dishes of 80% confluent Phoenix cells were transfected with 15 μg pBabe-puro-SR-IκB-α or pBabe-puro along with 5 μg of an Env-expressing vector. After 24 hours, the medium was changed, and cells were incubated for another 24 hours at 32°C to increase retrovirus half-life. Supernatants containing retrovirus were then harvested, filtered, and transferred onto rel-3983D target cells in the presence of 2 μg/mL polybrene (Sigma). Twenty-four hours after

infection, cells were washed, selected with complete medium plus 4 μg/mL puromycin for 4 days, and expanded in medium containing 1 μg/mL puromycin. Analysis of GFP expression indicated ~80% efficiency of retroviral infection of the rel-3983D cells (data not shown).

Results

DMBA promotes anchorage-independent growth and proliferation of rel-3983 cells. Cell lines were successfully established from three tumors from three independently isolated MMTV-c-*rel* mouse transgenic lines. Surprisingly, none of them were able to grow in soft agar. Given the expression of c-Rel in human breast cancer, we tested the ability of the prototypic PAH DMBA to promote a more mesenchymal phenotype for c-Rel–transformed breast cancer cells. The rel-3983 cells were treated with 10^{-6} mol/L DMBA or vehicle DMSO for 2 weeks, deriving the lines rel-3983D and rel-3983V, respectively. Cells were cultured and then tested for their ability to grow in soft agar. The DMBA-treated rel-3983D cells grew very effectively in soft agar forming large extensive colonies, whereas the parental rel-3983 cells and the vehicle-treated rel-3983V cells failed to form colonies (Fig. 1*A*). We next compared the growth rate of rel-3983 with rel-3983D and the untransformed mouse mammary cell line (NMuMG). Cultures, seeded in triplicate, were harvested after 1, 2, 3, 4, or 7 days, and cell numbers were determined. Both parental rel-3983 and rel-3983D mammary tumor cell lines displayed somewhat faster growth than the untransformed NMuMG mouse mammary cell line (Fig. 2). Between 2 and 4 days, it became apparent that the rel-3983D cells were growing substantially faster than the parental rel-3983. By 7 days, growth of the parental rel-3983 cells had leveled off, such that the numbers were equivalent to those of the NMuMG control cell line. In contrast, the DMBA-treated mouse tumor cell line continued to grow at a rapid rate, and by day 7, rel-3983D cell numbers were ~3-fold greater than those for parental rel-3983 or NMuMG lines

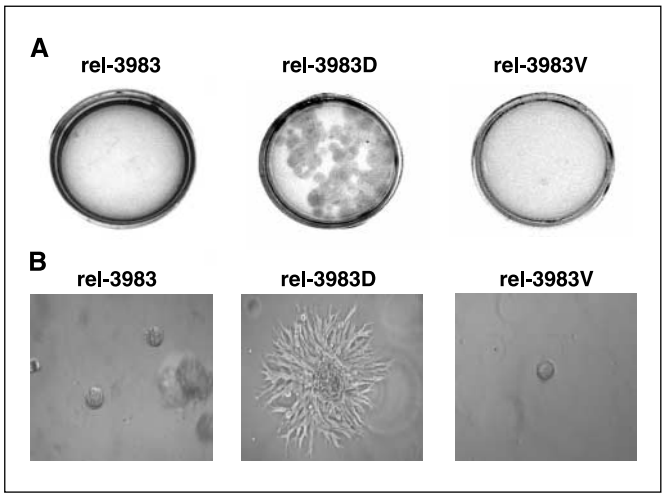

Figure 1. DMBA-induced rel-3983D cells display enhanced ability to grow in soft agar and Matrigel. *A,* cultures of rel-3983, rel-3983D, and rel-3983V cells were plated, in triplicate, in soft agar at a density of 5,000 cells per P35 dish. Plates were stained with crystal violet to visualize the cells and photographed using a Kodak digital camera. *B,* parental rel-3983, rel-3983D, and rel-3983V cells (5,000 cells) were plated, in duplicate, in Matrigel. After 3 days of incubation, the rel-3983D cells showed invasive branching pattern of growth in Matrigel, whereas rel-3983 cells yielded round colonies when examined. The plates were photographed using a Zeiss Axiovert 200M microscope and an Orca ER camera at ×50 magnification.

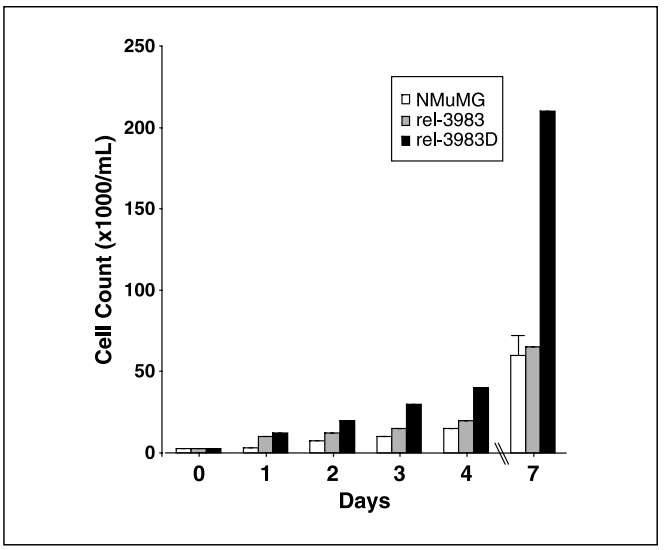

Figure 2. DMBA-treated rel-3983D cells grow more rapidly and achieve a higher density than rel-3983 cells. Cultures of rel-3983 and rel-3983D mammary tumor cells and untransformed NMuMG mammary epithelial cells were seeded, in triplicate, at 3,000/mL (day 0), and cell numbers were determined after 1, 2, 3, 4, or 7 days. *Columns,* mean; *bars,* SD.

(Fig. 2). Thus, DMBA treatment of rel-3983 cells resulted in a population of rel-3983D cells with a more transformed phenotype.

DMBA-induced rel-3983D cells form colonies with an invasive phenotype in Matrigel. EMT results in cells with a more invasive phenotype that are able to grow with extensive processes within Matrigel. Because the rel-3983D mouse mammary tumor cells showed a transformed phenotype as judged by growth in soft agar, we next assessed their ability to grow in Matrigel. The rel-3983D, rel-3983V, and control rel-3983 cells were plated in Matrigel. After just 1 day of incubation, short branches were seen in the DMBA-treated rel-3983D cells (data not shown), which became extensive by 3 days (Fig. 1*B*). In contrast, parental rel-3983 and rel-3983V cells were unable to grow in Matrigel over the time course. The Matrigel analysis indicates that rel-3983D cells have progressed to an invasive phenotype.

E-cadherin expression is reduced in rel-3983D versus parental rel-3983 cells. The invasive phenotype observed in DMBA-treated rel-3983D cells implied that the cells had lost/reduced E-cadherin expression (23). To address this hypothesis, indirect immunofluorescence microscopy was used to examine the levels of E-cadherin in the rel-3983 and rel-3983D cells. Cells grown on coverslips were incubated with an anti-mouse E-cadherin primary antibody followed by an Alexa 594 mouse secondary antibody. Following washing, the coverslips were mounted in Vectashield with DAPI to stain the nuclei. Shown in Fig. 3 are the individual and merged photos representative of two independent experiments. In rel-3983 cells (Fig. 3, *middle*), E-cadherin localized to the plasma membrane and at cell-cell junctions as previously described (23). However, in rel-3983D cells (Fig. 3, *bottom*), E-cadherin expression was decreased, as indicated by a significant decrease in the level of fluorescent staining.

NF-κB binding and subunit levels are induced in the rel-3983D cells. Aberrant constitutive NF-κB expression promotes a transformed phenotype (8, 16, 24). To assess the effects of DMBA-induced transformation on NF-κB expression in rel-3983D cells, nuclear proteins were isolated from rel-3983, rel-3983D, and

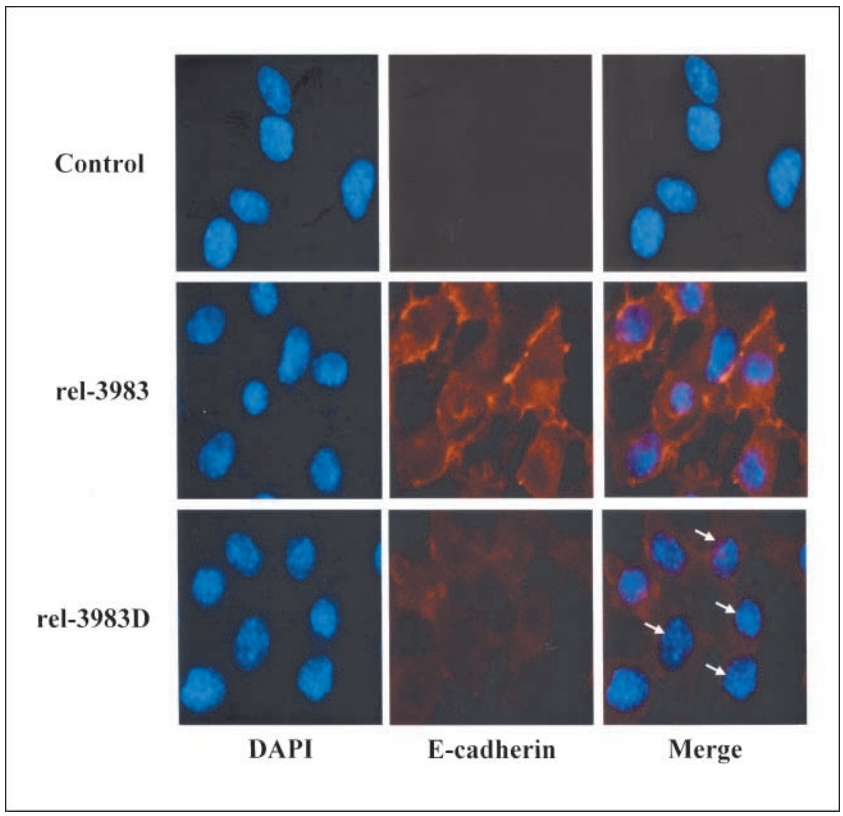

Figure 3. E-cadherin immunostaining is reduced in rel-3983D cells. The levels of E-cadherin in rel-3983 and rel-3983D were determined by indirect immunofluorescence microscopy using mouse anti-E-cadherin (primary) and Alexa 594 anti-mouse (secondary) antibodies. As control, no primary antibody was added. Nuclei were stained with DAPI. Fluorescence microscopy was done using a Zeiss Axiovert 200M microscope. Individual and merged images are shown.

rel-3983V cells and subjected to EMSA using the NF-κB element upstream of the c-*myc* promoter (ref. 20; Fig. 4*A*). Two major bands were seen in all of the extracts, which have been identified previously as p50/p50 homodimers and p50/RelA complexes. In addition, several minor complexes were seen with the rel-3983D cell extracts. The positions of migration of p50/c-Rel and p52/RelB complexes, previously identified by supershift EMSA (16, 25), are indicated. The level of NF-κB binding was clearly higher in the rel-3983D compared with either the parental or the vehicle-treated cells. Equal loading was confirmed by analysis of octomer-1 binding (Fig. 4*A*). Thus, NF-κB binding activity is higher in the rel-3983D cells than in the parental rel-3983 or vehicle-treated rel-3983V cells.

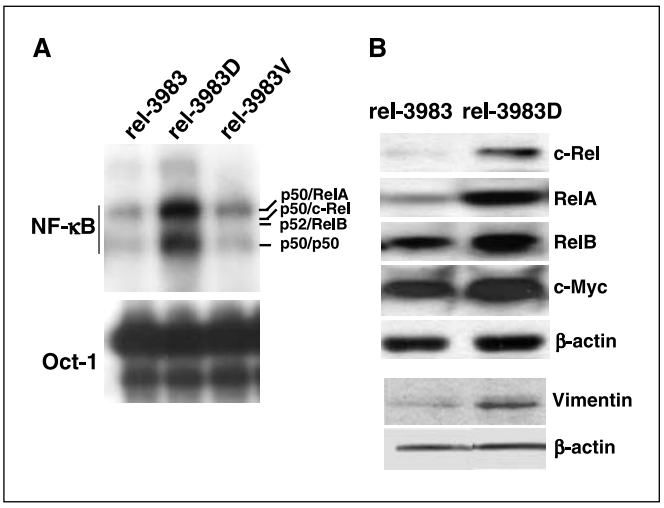

Figure 4. DMBA-treated rel-3983D cells display a higher level of NF-κB. *A,* nuclear extracts were prepared from rel-3983, rel-3983D, or rel-3983V cells, and samples (5 μg) were subjected to EMSA for NF-κB and octomer-1 (*Oct-1*), as loading control. The migration positions of p50/p50, p52/RelB, p50/c-Rel, and p50/RelA are as indicated. *B,* nuclear extracts were prepared from rel-3983 and rel-3983D cells, and samples (40 μg) were subjected to immunoblot analysis to determine the levels of the NF-κB subunits c-Rel, RelA, and RelB and the product of NF-κB target genes c-*myc* (c-Myc) and *vimentin*. As control, β-actin was used, which confirmed equal loading for the individual blots.

Because the mammary tumors that arose in the MMTV-c-*rel* mouse expressed multiple NF-κB subunits, we did immunoblot analysis for the three transactivating subunits: c-Rel, RelA, and RelB. Expression of c-Rel in rel-3983 cells was estimated at ~3.2-fold higher than that seen in wild-type virgin mouse mammary glands (data not shown). Higher levels of c-Rel, RelA, and RelB NF-κB subunits were detected in rel-3983D versus parental rel-3983 tumor cells (Fig. 4*B*). Essentially, equal loading was verified by analysis of β-actin levels. NF-κB target genes include the c-*myc* oncogene, which is overexpressed in mammary tumors in the MMTV-c-*rel* mice (16, 20), and *vimentin* (26). Immunoblot analysis detected a substantial increase in c-Myc levels in the rel-3983D cells compared with the parental rel-3983 cells (Fig. 4*B*). The level of vimentin was also elevated in the rel-3983D cells (Fig. 4*B*). These findings are consistent with the results of the EMSA, indicating functional NF-κB protein levels are higher in the rel-3983D cells than in the parental rel-3983 mouse mammary tumor cells.

Ectopic expression of SR-IκB-α slows proliferation and reverts invasive phenotype of rel-3983D cells. Given the roles of c-Myc, vimentin, and other NF-κB targets in control of proliferation and transformed phenotype, we tested directly the effects of inhibition of NF-κB on growth of rel-3983D cells using the specific inhibitory protein IκB-α. We used the pBABE retrovirus to deliver the super repressor SR-IκB-α variant, which cannot be phosphorylated and degraded (27), to the rel-3983D cells. As control, a pBABE vector expressing GFP was used. Cells were infected, then

selected with 4 μg/mL puromycin for 4 days, and expanded in medium containing 1 μg/mL puromycin. Expression of IκB-α was confirmed by immunoblot analysis (Fig. 5, *inset*). To test for the effects on growth, cells were plated as above, cultures were harvested after 1, 2, 3, 4, or 7 days, and cell numbers were determined (Fig. 5). SR-IκB-α–infected cells grew at a substantially slower rate, reaching a plateau by 7 days that resembled the parental rel-3983 cells.

Expression of functional NF-κB has been shown to be required for cells to maintain their invasive phenotype (24, 28). To test the role of NF-κB in the invasive phenotype of rel-3983D mouse mammary tumor cells, we tested the ability of rel-3983D-SR-IκB-α and rel-3983D-pBABE control cells to grow in Matrigel. After 3 days of incubation, rel-3983D-SR-IκB-α cells showed no growth, whereas the control rel-3983D-pBABE cells formed extensive invasive colonies (Fig. 6), comparable with the rel-3983D cells above. Taken together, these findings indicate that maintenance of NF-κB activity is required for the mesenchymal phenotype displayed by the rel-3983D mouse mammary tumor cells.

Discussion

Here, we show for the first time that the DMBA treatment of MMTV-c-*rel* mouse mammary tumor cells in culture results in EMT and show that NF-κB activity plays a crucial role in this process. Cell lines derived from tumors that arose in the MMTV-c-*rel* mouse all failed to grow in soft agar. DMBA-induced rel-3983D cells displayed an increased rate of proliferation, displayed growth to a higher cell density, and acquired an ability to grow in soft agar and in Matrigel compared with the parental rel-3983 or vehicle-treated rel-3983V cells. Rel-3983D cells showed a concomitant loss in E-cadherin expression and increase in expression of mesenchymal gene proteins vimentin and fibronectin (data not shown). Increased NF-κB binding activity and higher levels of c-Rel, RelA, and RelB were observed in rel-3983D cells versus parental rel-3983 cells. NF-κB activity seemed functional as judged by the induction of c-Myc and vimentin. Ectopic expression of SR-IκB-α confirmed the role of NF-κB in EMT of rel-3983D cells.

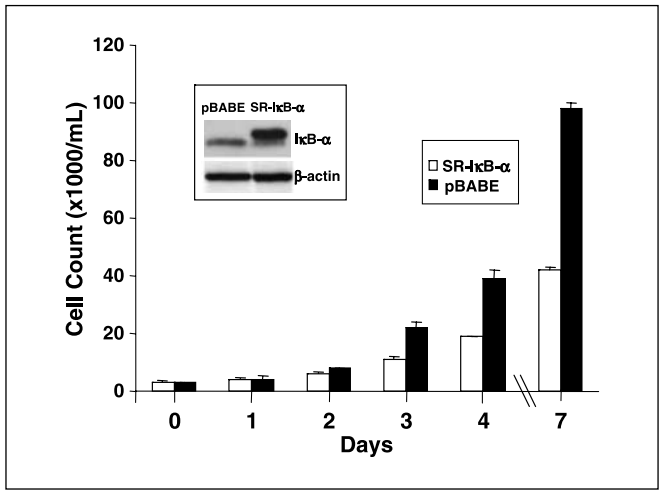

Figure 5. Ectopic expression of SR-IκB-α reduces rel-3983D proliferation. Cultures of rel-3983D mammary tumor cells were infected with pBABE-puro-SR-IκB-α or pBABE-puro, as control. Infected cells were selected using 4 μg/mL puromycin for 4 days and expanded in medium containing 1 μg/mL puromycin. *Inset,* whole-cell extracts were prepared, and samples (40 μg) were subjected to immunoblot analysis for IκB-α expression. For growth curve analysis, cells were seeded, in duplicate, at 3,000/mL (day 0), and cell numbers were determined after 1, 2, 3, 4, or 7 days. *Columns,* mean; *bars,* SD.

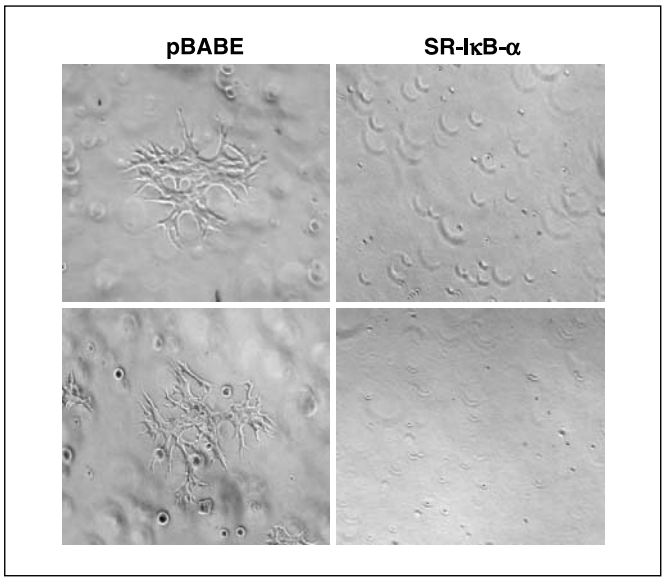

Figure 6. Ectopic expression of SR-IκB-α inhibits rel-3983D growth in Matrigel. Cultures of rel-3983D mammary tumor cells were transfected with pBABE-SR-IκB-α or pBABE-GFP, as a control. Cells were plated, in duplicate, in Matrigel and assessed after 3 days as described above in Fig. 1*B*. Two representative images are shown.

Thus, exposure to the carcinogen DMBA causes further activation of NF-κB and EMT of c-Rel–transformed breast cancer cells.

Ductal carcinomas *in situ* progress and acquire a more invasive, metastatic phenotype (29). NF-κB, which is known to regulate genes that promote cell survival and proliferation thus mediating neoplastic transformation (12, 13), has more recently been shown to be required for maintenance of EMT. Inhibition of NF-κB activity in EP-Ras XT mammary mesenchymal cells caused a reversal of EMT (28). Interestingly, oncogenic H-Ras, which signals via Raf/mitogen-activated protein kinase and phosphatidylinositol 3-kinase/Akt pathway, alters the normal response to transforming growth factor-β1 (TGF-β1) from growth inhibition or induction of apoptosis to EMT. Thus, whereas treatment of EpH4 untransformed mammary cells with TGF-β1 decreased their rate of growth, upon ectopic expression of activated H-Ras, TGF-β1 induced EMT (30, 31). Altered regulation of NF-κB seems critical to the resistance of Ras-transformed cells. We have shown that the decreased growth of breast cancer, hepatocyte, or rat liver epithelial (RLE) cells upon TGF-β1 treatment was due in part to a decrease in NF-κB activity, as ectopic expression of c-Rel led to the maintenance of NF-κB activity and resistance to TGF-β1–mediated inhibition of proliferation (32–34). In contrast, NF-κB binding and activity in Ras-transformed RLEs were resistant to TGF-β1, which failed to inhibit their rate of proliferation (34). Importantly, inhibition of NF-κB reduced their ability to grow in soft agar. Thus, NF-κB plays a critical role in TGF-β signaling pathways induced by oncogenic Ras that leads to EMT.

The c-Rel NF-κB subunit has been implicated in multiple human cancers. We observed that 86% of human primary breast tumor tissue samples express c-Rel (8), and Cogswell et al. obtained similar data (15). Amplification of the c-*rel* gene has frequently been observed in diffuse large cell lymphomas (35–37). Similarly, amplification or overexpression of c-Rel is displayed in Hodgkin's lymphoma, follicular large cell lymphoma, diffuse large cell lymphoma, and mediastinal B-cell lymphoma (12, 37). Furthermore,

50% of non–small cell lung carcinomas revealed elevated levels of c-Rel expression (38). Given our findings with the MMTV-c-*rel* transgenic mice (16), it is likely c-Rel plays an important role in the etiology of these cancers. Although DMBA does not naturally occur in the environment, our data suggest that polycyclic aromatic hydrocarbons within the environment have the potential to promote EMT via enhancement of NF-κB activity.

Acknowledgments

Received 8/25/2005; revised 12/16/2005; accepted 12/28/2005.

Grant support: NIH grant PO1 ES11624.

The costs of publication of this article were defrayed in part by the payment of page charges. This article must therefore be hereby marked *advertisement* in accordance with 18 U.S.C. Section 1734 solely to indicate this fact.

We thank A. Trombino for treating cultures with DMBA and R. Romieu-Mourez for generously providing the pBABE-puro-SR-IκB-α construct.

References

1. Morris JJ, Seifter E. The role of aromatic hydrocarbons in the genesis of breast cancer. Med Hypotheses 1992;38:177–84.
2. Willett W. The search for the causes of breast and colon cancer. Nature 1989;338:389–94.
3. Wolff MS, Toniolo PG, Lee EW, Rivera M, Dubin N. Blood levels of organochlorine residues and risk of breast cancer. J Natl Cancer Inst 1993;85:648–52.
4. Falck F, Jr., Ricci A, Jr., Wolff MS, Godbold J, Deckers P. Pesticides and polychlorinated biphenyl residues in human breast lipids and their relation to breast cancer. Arch Environ Health 1992;47:143–6.
5. Trombino AF, Near RI, Matulka RA, et al. Expression of the aryl hydrocarbon receptor/transcription factor (AhR) and AhR-regulated CYP1 gene transcripts in a rat model of mammary tumorigenesis. Breast Cancer Res Treat 2000;63:117–31.
6. Rogers AE, Conner BH. Dimethylbenzanthracene-induced mammary tumorigenesis in ethanol-fed rats. Nutrition Res 1990;10:915–28.
7. Calaf G, Russo J. Transformation of human breast epithelial cells by chemical carcinogens. Carcinogenesis 1993;14:483–92.
8. Sovak MA, Bellas RE, Kim DW, et al. Aberrant nuclear factor-kappaB/Rel expression and the pathogenesis of breast cancer. J Clin Invest 1997;100:2952–60.
9. Nakshatri H, Bhat-Nakshatri P, Martin DA, Goulet RJ, Jr., Sledge GW, Jr. Constitutive activation of NF-kappaB during progression of breast cancer to hormone-independent growth. Mol Cell Biol 1997;17:3629–39.
10. Kim DW, Sovak MA, Zanieski G, et al. Activation of NF-kappaB/Rel occurs early during neoplastic transformation of mammary cells. Carcinogenesis 2000;21:871–9.
11. Ghosh S, Karin M. Missing pieces in the NF-kappaB puzzle. Cell 2002;109 Suppl:S81–96.
12. Rayet B, Gelinas C. Aberrant rel/nfkb genes and activity in human cancer. Oncogene 1999;18:6938–47.
13. Sonenshein GE. Rel/NF-kappa B transcription factors and the control of apoptosis. Semin Cancer Biol 1997;8:113–9.
14. Romieu-Mourez R, Landesman-Bollag E, Seldin DC, et al. Roles of IKK kinases and protein kinase CK2 in activation of nuclear factor-kappaB in breast cancer. Cancer Res 2001;61:3810–8.
15. Cogswell PC, Guttridge DC, Funkhouser WK, Baldwin AS, Jr. Selective activation of NF-kappa B subunits in human breast cancer: potential roles for NF-kappa B2/p52 and for Bcl-3. Oncogene 2000;19:1123–31.
16. Romieu-Mourez R, Kim DW, Shin SM, et al. Mouse mammary tumor virus c-rel transgenic mice develop mammary tumors. Mol Cell Biol 2003;23:5738–54.
17. Thiery JP. Epithelial-mesenchymal transitions in tumour progression. Nat Rev Cancer 2002;2:442–54.
18. Sommers CL, Thompson EW, Torri JA, et al. Cell adhesion molecule uvomorulin expression in human breast cancer cell lines: relationship to morphology and invasive capacities. Cell Growth Differ 1991;2:365–72.
19. Wu M, Lee H, Bellas RE, et al. Inhibition of NF-kappaB/Rel induces apoptosis of murine B cells. EMBO J 1996;15:4682–90.
20. Duyao MP, Buckler AJ, Sonenshein GE. Interaction of an NF-kappa B-like factor with a site upstream of the c-*myc* promoter. Proc Natl Acad Sci U S A 1990;87:4727–31.
21. Pianetti S, Guo S, Kavanagh KT, Sonenshein GE. Green tea polyphenol epigallocatechin-3 gallate inhibits HER-2/*neu* signaling, proliferation, and transformed phenotype of breast cancer cells. Cancer Res 2002;62:652–5.
22. Romieu-Mourez R, Landesman-Bollag E, Seldin DC, Sonenshein GE. Protein kinase CK2 promotes aberrant activation of nuclear factor-kappaB, transformed phenotype, and survival of breast cancer cells. Cancer Res 2002;62:6770–8.
23. Kang Y, Massague J. Epithelial-mesenchymal transitions: twist in development and metastasis. Cell 2004;118:277–9.
24. Bachelder RE, Yoon SO, Franci C, de Herreros AG, Mercurio AM. Glycogen synthase kinase-3 is an endogenous inhibitor of Snail transcription: implications for the epithelial-mesenchymal transition. J Cell Biol 2005;168:29–33.
25. Currier N, Solomon SE, Demicco EG, et al. Oncogenic signaling pathways activated in DMBA-induced mouse mammary tumors. Toxicol Pathol 2005;33:726–37.
26. Lilienbaum A, Paulin D. Activation of the human vimentin gene by the Tax human T-cell leukemia virus. I. Mechanisms of regulation by the NF-kappa B transcription factor. J Biol Chem 1993;268:2180–8.
27. Brown K, Gerstberger S, Carlson L, Franzoso G, Siebenlist U. Control of I kappa B-alpha proteolysis by site-specific, signal-induced phosphorylation. Science 1995;267:1485–8.
28. Huber MA, Azoitei N, Baumann B, et al. NF-kappaB is essential for epithelial-mesenchymal transition and metastasis in a model of breast cancer progression. J Clin Invest 2004;114:569–81.
29. Vincent-Salomon A, Thiery JP. Host microenvironment in breast cancer development: epithelial-mesenchymal transition in breast cancer development. Breast Cancer Res 2003;5:101–6.
30. Miettinen PJ, Ebner R, Lopez AR, Derynck R. TGF-beta induced transdifferentiation of mammary epithelial cells to mesenchymal cells: involvement of type I receptors. J Cell Biol 1994;127:2021–36.
31. Oft M, Peli J, Rudaz C, et al. TGF-beta1 and Ha-Ras collaborate in modulating the phenotypic plasticity and invasiveness of epithelial tumor cells. Genes Dev 1996;10:2462–77.
32. Sovak MA, Arsura M, Zanieski G, Kavanagh KT, Sonenshein GE. The inhibitory effects of transforming growth factor beta1 on breast cancer cell proliferation are mediated through regulation of aberrant nuclear factor-kappaB/Rel expression. Cell Growth Differ 1999;10:537–44.
33. Arsura M, FitzGerald MJ, Fausto N, Sonenshein GE. Nuclear factor-kappaB/Rel blocks transforming growth factor beta1-induced apoptosis of murine hepatocyte cell lines. Cell Growth Differ 1997;8:1049–59.
34. Arsura M, Mercurio F, Oliver AL, Thorgeirsson SS, Sonenshein GE. Role of the IkappaB kinase complex in oncogenic Ras- and Raf-mediated transformation of rat liver epithelial cells. Mol Cell Biol 2000;20:5381–91.
35. Houldsworth J, Mathew S, Rao PH, et al. REL proto-oncogene is frequently amplified in extranodal diffuse large cell lymphoma. Blood 1996;87:25–9.
36. Barth TF, Dohner H, Werner CA, et al. Characteristic pattern of chromosomal gains and losses in primary large B-cell lymphomas of the gastrointestinal tract. Blood 1998;91:4321–30.
37. Gilmore TD, Kalaitzidis D, Liang MC, Starczynowski DT. The c-Rel transcription factor and B-cell proliferation: a deal with the devil. Oncogene 2004;23:2275–86.
38. Mukhopadhyay T, Roth JA, Maxwell SA. Altered expression of the p50 subunit of the NF-kappa B transcription factor complex in non-small cell lung carcinoma. Oncogene 1995;11:999–1003.

7,12-Dimethylbenz(*a*)Anthracene Treatment of a c-*rel* Mouse Mammary Tumor Cell Line Induces Epithelial to Mesenchymal Transition via Activation of Nuclear Factor-κB

Sangmin Ryan Shin, Nuria Sánchez-Velar, David H. Sherr, et al.

Cancer Res 2006;66:2570-2575.